STUDY OF BROADBAND PROPAGATION CHARACTERISTIC OF QUASI-FRACTAL PHONONIC CRYSTAL FOR ENHANCED SENSING APPLICATIONS

B. Figeys[1,2], R. Jansen[1], S. Severi[1], B. Nauwelaers[2], H.A.C. Tilmans[1], and X. Rottenberg[1]*
[1]Imec, Heverlee, BELGIUM
[2]ESAT, KU Leuven, Leuven, BELGIUM

ABSTRACT

This paper reports on bulk acoustic wave (BAW) resonators with quasi-fractal perforations for increased sensitivity in bio-sensing applications and on the broadband transmission line (TL) model of such resonators. Fractal perforations are implemented in BAW resonators to increase their surface area-to-volume ratio and to thereby enhance the sensitivity. We found that a further improvement is expected at higher resonance frequencies for the quasi-fractal phononic crystal (PnC) we have designed. This particular PnC has local resonances entailing strongly dispersive effective acoustic properties. Therefore, we have modeled the device implementing this PnC as a broadband dispersive transmission line (TL) to account for all the essential modes of longitudinal resonance. Our measurements, in very good agreement with this model, confirm the existence of the propagation mode in the PnC with enhanced projected sensitivity.

KEYWORDS

BAW resonant sensor, Phononic Crystal, TL model

INTRODUCTION

Bulk acoustic wave (BAW) resonators have been considered for a variety of applications such as filters [1], timing devices [1], IR imaging [2] and (bio)chemical sensors [3]. Recently, surface-micromachined resonators for sensing applications have been demonstrated [4], where the adhesion of mass on the resonator's surface leads to a shift in resonance frequency.

Previous research showed that the introduction of perforations in a BAW resonator can increase the sensitivity of the resonance frequency to mass adhesion in two ways [5]. Firstly, the total mass of the resonator decreases and, therefore, the adhesion of an equal amount of mass has a relatively larger impact on the resonance frequency. Secondly, the vertical walls of the perforations provide extra adhesion surface, which leads to an increase in the total adhered mass when the resonator thickness, indicated with T in Figure 1, is sufficiently large. In this paper, we therefore propose BAW resonators with quasi-fractal perforation shapes [6], as shown in Figure 2, for increased sensitivity due to a higher surface-area-to-volume ratio (SA/V). A further sensitivity-enhancement is possible at higher frequencies, due to the dispersive behavior caused by local internal resonances in the resonator medium. This dispersive medium can be regarded as an acoustic metamaterial (MTM) with frequency dependent effective acoustic properties [7].

Typically, resonators are modeled as RLC-equivalent circuits, where each mode of resonance requires its respective RLC branch. However, it has already been suggested that a transmission-line (TL) model can be used to represent a BAW resonator, including its harmonic resonances [8]. In order to model the different resonating modes of our BAW resonator, we successfully demonstrate the use of a *dispersive* TL model, as depicted in Figure 3, which represents all longitudinal resonances at once. In this model, the frequency dependence of the acoustic velocity is extracted from the band structure (BS) of the PnC.

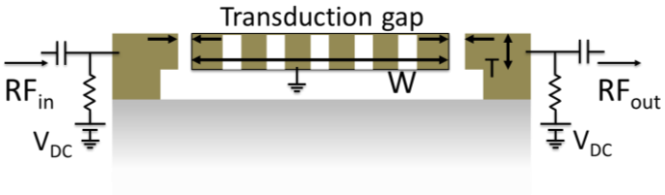

Figure 1: Electromechanical schematic cross-section of the proposed resonator.

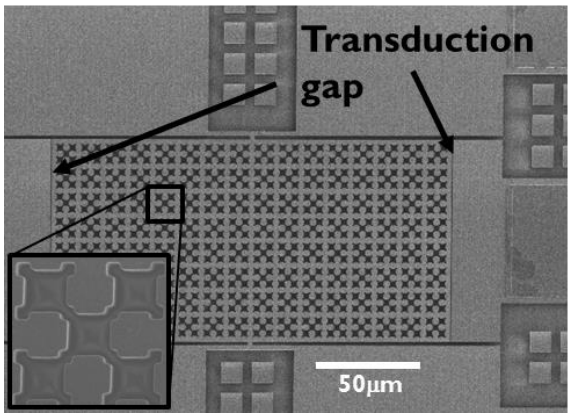

Figure 2: SEM picture of a BAW resonator with quasi-fractal perforations in SiGe. Inset shows the unit cell of the PnC.

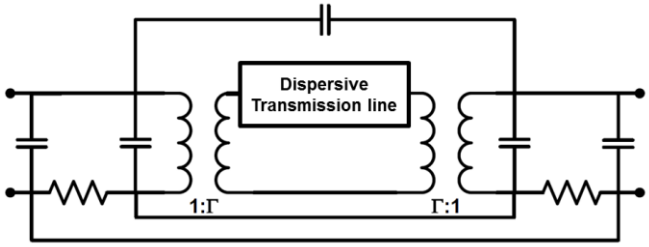

Figure 3: Broadband model of a BAW resonator with a dispersive TL to model the resonator in Figure 2.

DESIGN OF RESONANT SENSORS

We have designed and fabricated a variety of rectangular shaped BAW resonators in imec's SiGe-MEMS technology. These devices are electrostatically actuated and sensed via a 500nm transduction gap, as is shown in Figure 1. At resonance longitudinal acoustic waves form a standing wave in the width W of the device. The propagating medium of the acoustic wave consists of an array of perforations that can be modeled as an acoustic metamaterial with an effective longitudinal velocity that can be extracted from a unit cell of the PnC.[9] We have studied the projected sensitivity of the different resonator designs for both their ground mode, and their harmonic resonance modes, and this will be discussed in the following subsections.

Sensitivity of the first width-extensional mode

In order to study the effect of the SA/V ratio, we designed resonators with equal footprint, varying by their perforation sizes and shapes as shown in Figure 4. To compare these, we use the sensitivity to adhered mass per unit area defined as:

$$\text{Sensitivity } S_{mass} := \frac{1}{f_0} \cdot \frac{\partial f_0}{\partial \rho_s}, \quad (1)$$

where f_0 is the resonance frequency and ρ_s is the mass per unit surface that adheres homogeneously on all accessible surfaces of the resonators. Hence, from (1), we can deduce that for low frequencies, in which the quasi-static evaluation of the effective density is valid, the sensitivity is proportional to the SA/V ratio:

$$\text{Quasi-static } S_{mass} = -\frac{1}{2} \cdot \frac{SA/V}{\rho_0}. \quad (2)$$

where ρ_0 is the mass density of the material (SiGe). The SA/V ratio can be increased by decreasing the thickness of the layer, by increasing the perforation size, or by reducing the perforation pitch [5]. To explore this, we have proposed (quasi-)fractal perforations for increased SA/V ratio. The SA/V ratios of the structures in Figure 4 normalized to the SA/V of a resonator of equal thickness (4µm) and footprint but without perforations are 1.08 (a), 1.66 (b), 2.66 (c) and 2.91 (d), as it can be calculated from Figure 5. The structures with higher SA/V will be more sensitive to adhered mass.

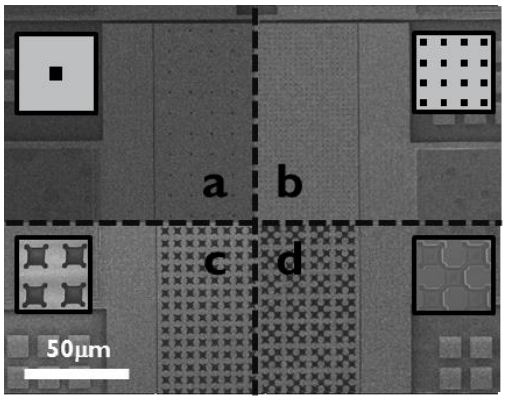

Figure 4: SEM pictures of fabricated devices with increasing SA/V and therefore increasing sensitivity.

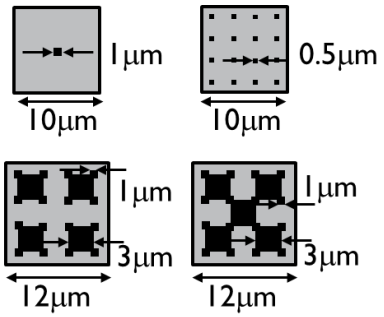

Figure 5: Dimensions of devices shown in Figure 4. The out-of-plane thickness T is 4µm.

Sensitivity of higher order modes

The projected sensitivity of harmonic resonances has been studied for the structures shown in Figure 4d and Figure 2. The propagation medium of these resonators is highly dispersive as can be seen from the band structure shown in Figure 6 that only depicts the relevant longitudinal modes of propagation. The dispersion in the band structure is caused by two low-frequency resonance modes at 57MHz and 106MHz, which are shown in the outsets of Figure 6. This can be recognized as typical for acoustic metamaterials with local resonances, i.e. the effective mass density of this medium will increase close to resonance around 50MHz, causing an increase in the acoustic velocity of propagation.

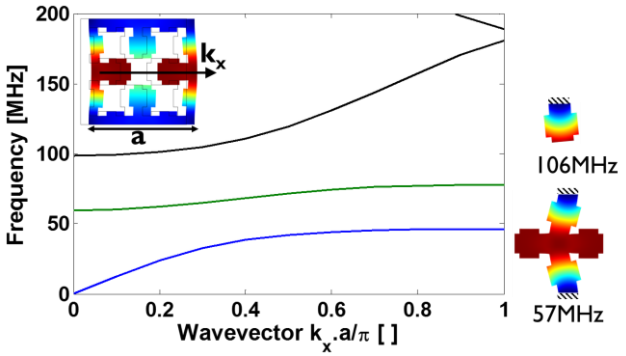

Figure 6: Band structure of the PnC defined by the unit cell of Figure 4d. Inset shows simulated result with COMSOL Multiphysics of a propagating mode on the blue line. The outsets show the local resonance that give rise to the band gaps around 50MHz and 100MHz. Colors: horizontal displacement.

The quasi-static model used for (2) is no longer valid when the effective mass density of the material becomes frequency dependent. Therefore, these devices require a dynamic analysis to extract the sensitivity of the harmonic resonances. In order to evaluate the sensitivity, we quantify the impact of adhered surface mass on the band structure of the PnC, as it is shown in

Figure 7 (dotted lines), and subsequently use (1). This has been done for the PnC structures proposed in Figure 4, with SiGe material properties (Young's modulus E_0 = 130GPa, Poisson's ratio ν_0 = 0.22 and mass density

ρ_0 = 4400kg/m^3). The extracted sensitivities, normalized to a slab of equal thickness (4μm) without perforations, are shown in Figure 8. The normalized sensitivity for the devices with unit cells *a*, *b* and *c* of Figure 4 does not vary with frequency at low frequencies, i.e. wide resonators, and it is equal to the aforementioned normalized SA/V. In contrast, the acoustic MTM shown in Figure 4d exhibits an enhanced sensitivity with increasing frequency, which is due to the sensitivity of the local resonances to mass. This is especially noticeable in the green mode shown in Figure 8, where a remarkable increase in sensitivity of up to 50% is expected as compared to its SA/V ratio.

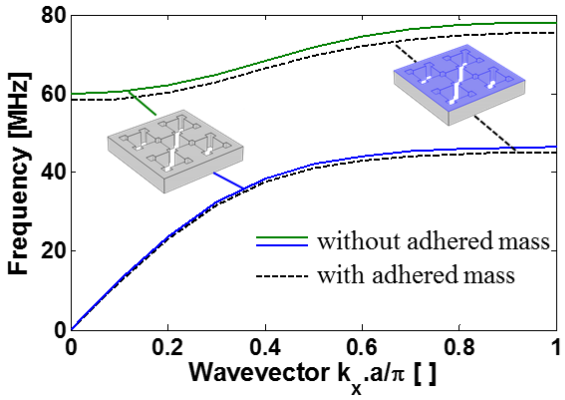

Figure 7: Effect of surface mass on PnC. The solid lines represent the device without adhered mass. The dotted lines are slightly shifted curves because of the added surface mass on the accessible area of the resonator, indicated in blue in inset.

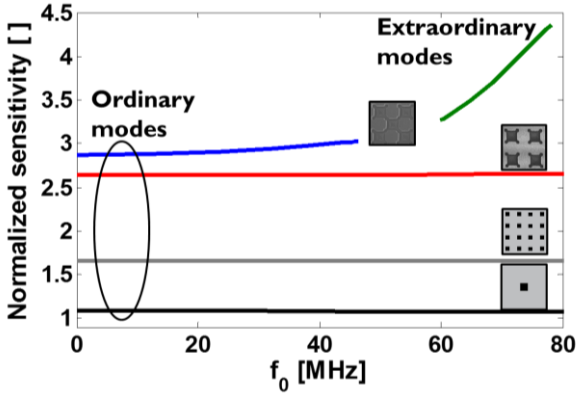

Figure 8: Projected normalized sensitivity vs resonance frequency f_0. For different designs of Figure 4 and different order of the modes.

BROADBAND TL MODEL VERIFICATION

In our previous calculations, we have used the band structure of the dispersive quasi-fractal PnC of Figure 2 as the input for the mass sensitivity analysis. In order to demonstrate that the band structure predicts the different harmonic resonances and that it, therefore, can be used for the sensitivity analysis, we have fabricated a very wide – large W – resonator (Figure 2), which has been characterized in a broad range of frequencies. Figure 9 shows some typical S_{21}-measurements of the device shown in Figure 2, which have been measured in vacuum with a DC bias voltage of 60V.

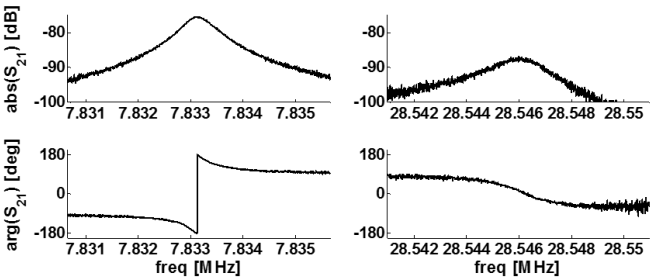

(a) 1 node (b) 4 nodes

Figure 9: Typical measurement for low/high (a/b) Rm devices. V_{DC}=60V and Q ~13k. Here are shown resp. 1st and 4th order modes of Fig. 1.

With these measurements, it is possible to reconstruct the band structure by assigning to each resonance its corresponding wavevector k_x, as shown in Figure 10, according to:

$$\frac{k_x.a}{\pi} = N.\frac{a}{W}, \qquad (3)$$

where *W=16a* for the *N*th harmonic resonance, corresponding with *N* nodes in the resonance mode. These results show a good match between measurements and simulations, which validates the methodology used in the previous section. However, as shown in Figure 11, the motional resistance *Rm* increases with frequency, which decreases the resonance amplitude until almost disappearing in the noise. The challenge, then, is to overcome the high Rm of the high frequency modes in order to enable the enhanced sensitive mode shown in Figure 8 (green).

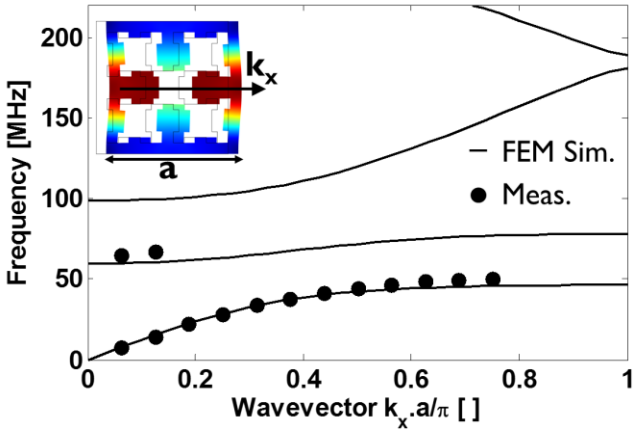

Figure 10: Band structure (BS) of longitudinal modes of the PnC. Solid lines show the BS as simulated with COMSOL Multiphysics, see inset. Dots are measurement points positioned on their rightful place, according to Equation 3. Colors: horizontal displacement.

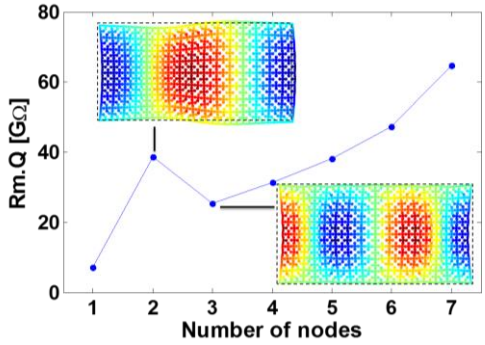

Figure 11: From measurement extracted Rm.Q, at V_{DC}=60V. Insets show eigenmodes for 2 and 3 nodes in the resonator, resp. at 15MHz and 22MHz. Colors: horizontal displacement.

The results shown in Figure 10 also suggest that we can use a TL as broadband model of the resonator. However, it is important to use a *dispersive/MTM*–TL in order to include the dispersive acoustic properties of the PnC. From Figure 12, we can conclude that it is possible to model the successive harmonic resonances of Figure 10 in Advanced Design System (ADS), using only one dispersive TL with the right length and phase velocity, as extracted from the PnC in Figure 6. This in contrast to the RLC-models, where a different RLC branch has to be implemented for each harmonic resonance . Therefore, this dispersive TL approach simplifies significantly the broadband modeling of BAW resonators. Currently, an arbitrary 0.5MΩ impedance is used, as an effective impedance extracted from a unit cell is not yet included in our MTM-TL model.

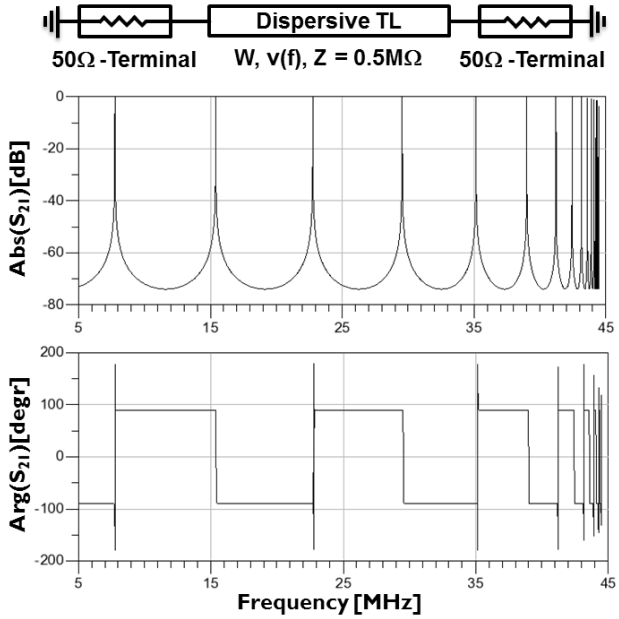

Figure 12: With Advanced Design System (ADS) simulated S_{21} parameters (bottom) of a dispersive TL (top) with a dispersive phase velocity v(f) extracted from the BS of Figure 6, fixed length corresponding to the width W of the resonator and an arbitrary 0.5MΩ impedance to provide reflections.

CONCLUSION

We designed and characterized BAW resonators with quasi-fractal perforations of increased SA/V, which exhibit higher predicted sensitivities to surface-mass adhered on the accessible faces of the resonator. The array of quasi-fractal perforations enables local resonances in the devices, inducing potentially highly-sensitive resonance modes. We demonstrated that it is possible to model all harmonic resonances of these devices with just one dispersive TL.

REFERENCES

[1] C.T.-C. Nguyen, "MEMS technology for timing and frequency control," *IEEE Transactions on Ultrasonics, Ferroelectrics, and Frequency Control*, vol. 54, no. 2, pp. 251–270, Feb. 2007.

[2] J. R. Vig, R. L. Filler, and Y. Kim, "Uncooled IR imaging array based on quartz microresonators," *Journal of Microelectromechanical Systems*, vol. 5, no. 2, pp. 131–137, Jun. 1996.

[3] P. S. Waggoner and H. G. Craighead, "Micro- and nanomechanical sensors for environmental, chemical, and biological detection," *Lab Chip*, vol. 7, no. 10, pp. 1238–1255, Sep. 2007.

[4] S. Lenci, F. Pieri, L. Haspeslagh, J. De Coster, S. Decoutere, A. Maestre Caro, S. Armini, and A. Witvrouw, "Stiction-free poly-SiGe resonators for monolithic integration of biosensors with CMOS," in *Solid-State Sensors, Actuators and Microsystems Conference (TRANSDUCERS), 2011 16th International*, 2011, pp. 2136–2139.

[5] X. Rottenberg, R. Jansen, V. Cherman, A. Witvrouw, H. A. C. Tilmans, M. Zanaty, A. Khaled, and M. Abbas, "Meta-materials approach to sensitivity enhancement of MEMS BAW resonant sensors," in *2013 IEEE SENSORS*, 2013, pp. 1–4.

[6] N.-K. Kuo and G. Piazza, "Ultra high frequency air/aluminum nitride fractal phononic crystals," in *Frequency Control and the European Frequency and Time Forum (FCS), 2011 Joint Conference of the IEEE International*, 2011, pp. 1–4.

[7] Z. Liu, X. Zhang, Y. Mao, Y. Y. Zhu, Z. Yang, C. T. Chan, and P. Sheng, "Locally Resonant Sonic Materials," *Science*, vol. 289, no. 5485, pp. 1734–1736, Sep. 2000.

[8] X. Rottenberg, R. Jansen, and H. A. C. Tilmans, "Phononic Bandgap coupled Bulk Acoustic wave Resonators," in *2012 IEEE 25th International Conference on Micro Electro Mechanical Systems (MEMS)*, 2012, pp. 725–728.

[9] X. Rottenberg, R. Jansen, C. Van Hoof, and H. A. C. Tilmans, "Acoustic meta-materials in MEMS BAW resonators," *Applied Physics A: Materials Science & Processing*, vol. 103, pp. 869–875, Jun. 2011.

CONTACT

*B. Figeys, tel: +32 16283553; Bruno.Figeys@imec.be